Indian Journal of Science and Technology, Vol 8(20), DOI: 10.17485/ijst/2015/v8i20/79147, August 2015
ISSN (Print) : 0974-6846
ISSN (Online) : 0974-5645

Image Discrimination of Human's Visual Perception for Thought Translational Device

Eric Tiong Kung Woo, M. P. Paulraj* and Abdul Hamid Adom

School of Mechatronic Engineering, University Malaysia Perlis, Pauh, Malaysia; paul@unimap.edu.my

Abstract

Electroencephalography (EEG) signal is a biological signal which can be associated to the mental task of a person. A Brain-Computer Interface (BCI) can be designed such that the mental activity accounted for the visual perception of a person can be recorded and subsequently converted into a control signal for controlling the movement of a wheelchair. Comparison was made between the Multi-Layered Perceptron feed-forward network (MLP) and Nonlinear Autoregressive Exogenous model (NARX) as a variant of Recurrent Neural Network (RNN). The networks were designed to discriminate the different brain activities when the subject was being presented with different visual stimuli. The trained network models have yielded an average accuracy of 93.3% for MLP models and 98.1% for NARX models.

Keywords: Brain Computer Interface (BCI), Electroencephalography (EEG), Levenberg-Marquardt Training Algorithm (LM), Multi-Layered Perceptron Neural Network (MLP), Nonlinear Autoregressive Exogenous Model (NARX), Power Spectral Density (PSD), Visual Perception

1. Introduction

Brain Computer Interface (BCI) provides its users a communication channel that does not depend on the brain's output through the nerves and muscles[1,2]. In other words, BCI let humans communicate or interact with the world without depending on muscular activities[3]. Development of such a technology proved invaluable for those suffering from motor neuron impairments[2-4] or otherwise, known as a group of diseases call Motor Neuron Disease (MND). Patients with MND, including those suffering from celebral palsy or amyotrophic lateral sclerosis are known as lock-in patients, where they can still be fully aware of their surroundings but having severely limited abilities to respond or interact with it[5].

As no known cure for ALS was found, efforts have been shifted in search of effective ways of treatment to the disease[6]. Hence, BCI provides an alternative solution to improve or overcome the limitations of MND patients. BCI enables lock-in patients to communicate with the physical world, thus compensating their psysical constrainments[7-9]. Attempts to design intelligent wheelchairs with automated control system thus far have been promising, which provided navigational aid for these groups of patients[10-12].

Robotic wheelchair can be categorized under rehabilitation and assitive technology in attempt to restore the lost of human ability due to disabilities, diseases, injury or aging[13]. In relation to the subject, a survey was done among clinicians where 91 percent of them believed that robotic wheelchair with automated navigational system might be useful for some of the patients[14]. Hence, it was explicitly stated that a wheelchair with high level of autonomy helps to aid the Differentially Enabled (DE) communities with their day-to-day tasks.

Interfaces of BCI includes invasive implants[7], partially invasive implants (Electrocorticography (ECoG))[7,40] non-invasive electrodes (Electroencephalography (EEG))[7,8,10-12,15-17] and Magnetic Resonance Image (MRI)[7,15]. Among those, EEG is the most frequently studied of the BCI interfaces due to its simplicity in its application, higher cost efficiency and portability. EEG is first recorded in 1924 by Hans Berger[7,18]. Since its discovery, clinical approaches had been developed in the diagnostics

*Author for correspondence

and treatment of neurological disorders such as epilepsy[17] and elliptic seizure[20,40].

EEG signals can be observed as oscillatory spikes of potential difference on specific points on the scalp, indicating the cranial activity of a person associated to a mental task. Electrical activity recorded by electrodes placed on the scalp or surface of the brain mostly reflects summation of excitatory and inhibitory postsynaptic potentials in apical dendrites of pyramidal neurons in superficial layers of the cortex[19], indicating the flow charge carriers (Na^+, K^+, Ca^{++} and Cl-ions) that results in electrical brain activity[30].

Though, EEG tends to be less effective than its more invasive counterparts by having less signal clarity. EEG signals[7]. EEG signals normally would have lower signal to noise ratio as electrode used to measure the potential difference is placed directly on the scalp of its user[18] instead of reading the signal at the brain itself. EEG signals representing the brain activity are known to be heavily contaminated with non-cortical biological artifacts (e.g.: eye movements, muscle movements and heartbeats) and environmental noise (power line noise and electromagnetic interference)[18]. On top of that, EEG signals are inherently stochastic in nature by having non-stationary properties[17,28]. This needed to be taken into account while designing feature extraction methods as frequency which holds information regarding the brain activity would change over time.

It is known that the five senses of MND patients (sight, hearing, taste, smell and touch) are not affected by the disease[13]. Hence, stimuli from human sense can be recorded as EEG signals and used to determine the mental task associated to the task. Investigation on both visual perception event-related and steady state responses have being made in relation to the subject[26]. A research was done by Dentico, Daniela, et al. on the relationship of visual perception and visual imagery. Their research highlighted the regions of a brain involved in visual perception and visual imagery while pointing out that the information simply flow in a reverse direction while comparing between visual perception and visual imagery[27].

Kyung Hwan Kim and Ja Hyun Kim investigated the gamma-band activity of a person while perceiving characters of different languages (Korean, Chinese and English)[21]. Analysis of variance (ANOVA) of gamma wave's band power was used as features in their research. Likewise, Aliette Lochy, Goedele Van Belle and Bruno Rossion used human visual perception to classify words, pseudo-words, non-words and pseudo-fonts which were presented as visual stimuli to the subject[22]. Z-scores were calculated for the signal in frequency domain to determine the channels that holds statistical significant response.

Effort was also made to investigate the effectiveness of implementing visual perception on an automated wheelchair. Itturate et al designed an automated wheelchair that relies on a BCI that reads the subject's attention on different points of an image[13]. Images being displayed were virtual reconstrcutions of the user's immediate surroundings. Such BCI system requires less human intervention by having higher level of autonomy[10].

Neural networks are known to be used as classifiers for associating EEG signals that represents different mental tasks. Neural networks are designed to imitate the behavior of biological neurons where each learning iteration strengthens the connections between the neurons involved. Similarly, Artificial Neural Network (ANN) operates with a basic principle that connection between two neurons, which is represented as a weight value is strengthened accordingly while both the neurons are excited simultaneously. One of such rules used in learning is Hebbian rule[23].

Neural network is known to be a self-optimizing model which 'learns' the pattern by adjusting itself to the data presented, without explicit mathematical or distributional specifications on the sets of features that the network model is supposed to learn. This means that the network is designed to be a universal approximation to any given function[29]. On top of that, most ANN, for instance, Multi-Layered Perceptron (MLP) works well with non-linear problems, which coincides with the fact that most complex real world models are non-linear[25].

Hema et al. demonstrates the use of band power of different channels of EEG signals, namely, α (6Hz-12Hz), β (12Hz-30Hz), γ (31-70Hz) and θ (4Hz-6Hz) as features to be used in classifying EEG signal in their research. A Recurrent Neural Network (RNN) was used as a classifier[24]. Their work yielded an accuracy of over 90 percent. Similar research was performed by Naderi and Homayoun such that a Recurrent Neural Network was designed to detect epileptic seizure in a subject by using features of EEG signals. Comparison between MLP and RRN was made where the results shows slightly higher accuracy of the RRN architecture compare to that of the MLP.

Recurrent Neural Network is known to perform well with time series problems, particularly where the signals that demonstrates stochastic behavior. Number of research

works has been made to show the efficacy of these models employed with time variant function in the analysis of biological signals. Hiroka Kato et al. demonstrate the performance of different variants of autoregressive models on electrophysiological signals. In their research, ECoG and EMG signals are used to determine the quality of different autoregressive models[41].

2. Methodology

2.1 Experimental Design

The goal of this research is to determine a suitable network model to classify and learn the discrimination process in relation to the visual perception of a subject when the subject is being presented with different visual stimuli (images). The BCI system should be able to translate the visual perception recorded from the subject, whereby the BCI is able to know which image was shown to the subject.

Five pictures as shown in Figure 1, representing five different places in a house were being displayed to the subject for 8 seconds each. These images were being compiled into a video and was played in a sequential order. The subjects were then requested to concentrate on the center of the screen for a period of 8 seconds. The center of the screen was indicated by a '+' sign, being displayed to the subject before each image appeared onscreen. EEG signals were recorded while the subjects were perceiving the images.

2.1.1 Equipment and Instrumentations

Figure 2 shows the setup for data collecting session wherein the Mindset-24 EEG amplifier is used to amplify the EEG signals. The EEG amplifier was connected to a EEG electrode cap (holding 19 channel electrodes), which was designed according to 10-20 electrode placement system as indicated in Figure 3 (the 19 channel does not include

Figure 1. 5 pictures of different locations in a house being displayed to the subject.

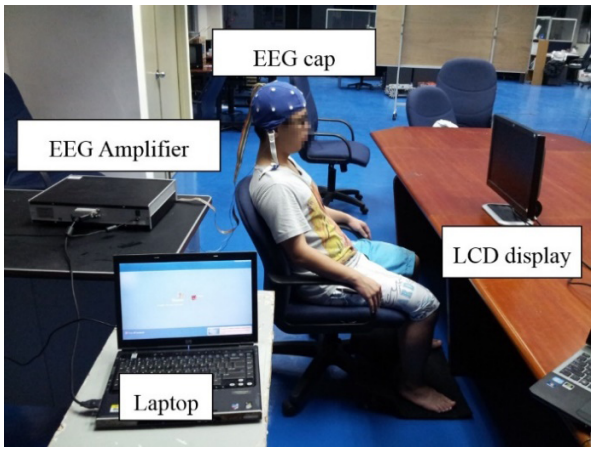

Figure 2. Experimental setup for recording the EEG signal with instruments including: 19-channel EEG amplifier (Mindset-24), 19-channel EEG cap, laptop with preinstalled program to interface with the EEG amplifier and 15.6 inch LCD display with native resolution of 1920x1080 pixels.

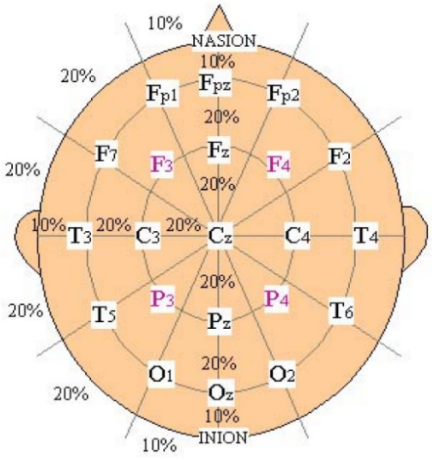

Figure 3. 10-20 system for electrode placement on the human scalp[30].

channels for both Fpz and Oz). A laptop with pre-installed interface software (mind meld) is used to record the EEG signals. The analog signals are then being encoded and stored in a digital medium[30]. A 15.6-inch LCD display is used to play the video to the subject while EEG signals were being recorded. The recorded signal was then being processed with Matlab software.

2.1.2 Data Acquisition

Subjects for the experimental study were selected among voluntary UniMAP students (10 subjects), aged between 18 to 30 years old of both gender. All the selected subjects

were examined by physicians and ensured that they were sound and healthy while not being affected by any diseases involving their central nervous system. Prior data collecting sessions, subjects were advised to sleep and rest well, take normal food and avoid any stressful activity.

During the signal recording session, the subjects were seated comfortably in front of a LCD display with a distance of 0.6 m of screen-to-eyes distance. This arrangement thus ensures that the subject's maximum numbers of light sensitive cones in the eyes are activated by the images shown on the screen. A large portion of these light sensitive cones lies within a 10° radius from the center of each eyes[31]. The subject was then requested to adjust the screen's brightness setting to reduce the stress caused by the screen's radiation to the subject's eyes. This arrangement is to reduce the frequency of blinking of the subject which might reduce the accuracy of the results.

EEG signals were recorded for 8 seconds at a sampling frequency of 256 Hz for all the 19 channels of EEG signals while the subjects perceived the video. For each task, eight trails were made and the same experimental procedure was repeated for five different tasks where the subject was requested to identify a different location of in a house each time.

2.1.3 Data Preprocessing

The EEG signal was first normalized by dividing the sampling signal, f(t) by its total mean value across the entire period of 8 seconds for each tasks and channels involved so as to remove signal offset. f_{norm} in the equation below is the normalized signal while t is the time domain of the signal.

$$f_{norm}(t) = \frac{f(t)}{\sum_{t=1}^{N} f(t)} \quad (1)$$

Next, an elliptic filter was used to remove the noise and artifacts from the signal. By setting the cut-off frequency at 50 Hz, power line noise was removed[18]. Band pass filters were designed of size: α band (6 Hz-12 Hz), β_1 band (12Hz-16Hz), β_2 band (16Hz-20Hz), β_3 band (20 Hz-28 Hz), γ_1 band (31 Hz-40 Hz) and γ_2 band (41 Hz-75 Hz) to extract the prominent features.

2.1.4 Feature Extraction

Since EEG signals are stochastic in nature, it is required to represent them in time-frequency domain so that the change of frequency across time can be observed. Short-Time Fourier Transform (STFT)[28] is used to preform Fourier Transform instead of conventional Fast Fourier Transform (FFT). STFT performs discrete Fourier transform along the time signal which is being divided into frames of segments. This can be done by having a window where the length of the window will determine the time resolution preserved after performing STFT. The window size is set to be small as in a shorter change of time EEG signals can be more closely represented as a stationary signal.

STFT was applied by performing Fourier transform for every 0.5 seconds of signal. A rectangle window function with length of 1 second and 50 percent of overlapping for each window was used as a frame for the segmentation of signal into its sub segments. This means that STFT retains a low-resolution time information where the change in band power across 8 seconds of recording can be observed in a resolution of 1.875 band power representations per second. Hence, we have an input vector, consisting of 520 samples for every band and channel of EEG signal.

P in Equation 2 is the power spectral density of the EEG signal. f(ω) in Equation 2 and 3 are the signals in frequency domain with ω indicates frequency component whereas f(t) in Equation 3 indicates the signal in time domain, with t as the time component. W in Equation 2 corresponds to the sampling frequency divided by 2 while performing Fourier transform. t_1 and t_2 indicates the upper and lower limits of the window used to perform STFT, with t_2 minus t_1 equals to the size of the window.

$$P = \lim_{W\to\infty} \frac{1}{2W} \int_{-W}^{W} |f(\omega)|^2 d\omega \quad (2)$$

$$F(\omega) = \frac{1}{2\pi} \int_{t_1}^{t_2} f(t) e^{-j\omega t} d\omega \quad (3)$$

2.1.5 Classification: Multi-Layered Perceptron Network Model

MLP network model remains the most popular network model as it can be trained with a large number of training algorithms including supervised, unsupervised and reinforced learning[32]. Error Back-Propagation (EBP) is the most frequently used of all training algorithms. EBP incorporates the delta learning rule and the gradient descent technique[23,33] to back-propagate the error the

connecting neurons in its previous layer determine the error contributed by a specific neuron towards the total error in the output neurons. Errors are determined by the difference between the output and the target.

Figure 4 shows the basic structure of a MLP network model. The input layer (of X_n neurons) is connected to output layer (of Y_m neurons) through the hidden layer(s) (Z_o). Subscripts n, m, o indicates the number of neurons in its respective layer. The strength of connection between neurons in different layers is indicated by its weight value between two neighboring neurons. As input vector, **S** was presented the network, it passes through layers of non-liner elements (neurons with activation function modeled after the firing rate of biological neurons) which resulted in slower leaning[23,34,35].

Hence, Levenberg-Marquardt (LM) algorithm was chosen as the training algorithm to train the MLP architecture. LM training algorithm incorporates gradient descent method with Newton-Gaussian method to reach the minimum of an error gradient. LM's main advantage over EBP is its ability perform faster training compare to EBP training algorithm[23,34-37]. Thus, LM algorithm can achieve the better accuracy in its results with lesser epochs of training.

$$S = [x_1, x_2, \ldots x_n] \quad (4)$$

Considering the non-stationary property of EEG signal, a RRN can be used as a pattern classifier. RRN performs well when classifying features of a system with dynamic behavior. Contrast to the feed-forward network structure, RRN is a combination of feed-forward and feed-back network model where the current output (t) can be used as a feature to predict the next output (t+1), as indicated in Figure 5. The current input is denoted as u(t) while y(t) is the output of the network. The network also contains a self-feedback loop with a delay where both u(t+1) and y(t) are used to predict the output of y(t+1). While training the network with back-propagation, the network can be unfolded across time to obtain the error contribution of the previous time states towards the current output.

The RNN model proposed in this research is of type NARX model. The basic structure of the NARX model is shown in Figure 6. It is simply an autoregressive model with a time varying process wherein the output values depend on the previous states of the system. The output equation of the structure is shown in Equation (5)[40]. y(t)

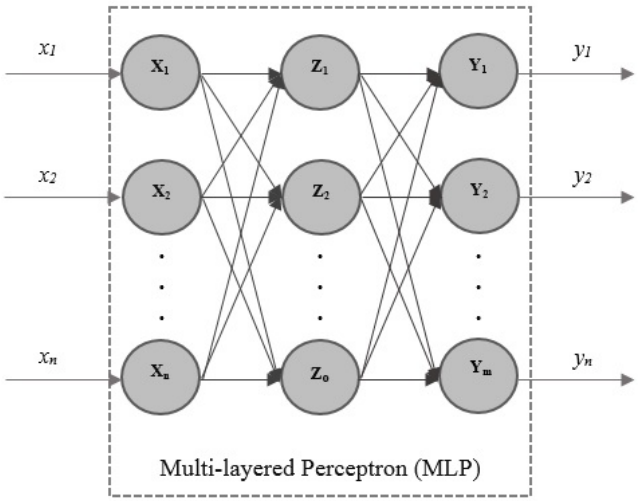

Figure 4. Basic structure of a MLP neural network model.

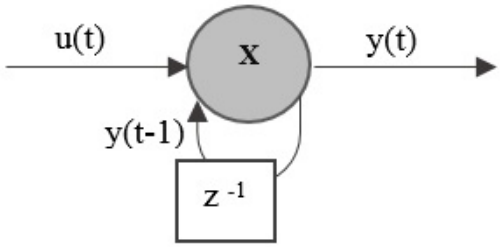

Figure 5. A single layered Single Input Single Output (SISO) RNN structure.

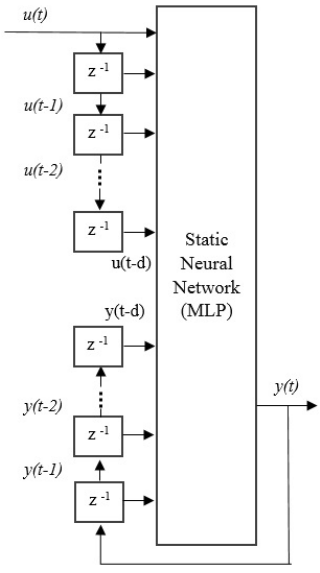

Figure 6. Basic structure of a NARX neural network model[42].

is the output of the system, t denotes the current state, C is the model's constant, ϕ is the functional parameter of the signal and $\varepsilon(t)$ is the random noise of the signal. From Equation 5 we have the elements to modify the recurrent neural network such that the inputs of the current instance and the delayed input from the previous instances, as well as the delayed output from the previous instances are used to predict the current output and the associated equation is Equation 6. In Equation 6, y(t) is the current output, u(t) is the current input and d denotes the delay in the system.

NARX network model can be trained with any standard training algorithm that can be use to model MLP network without modifications since feedbacks are stored in context nodes through layer(s) of delay(s).

$$y(t) = C + \sum_{i=1}^{P} \varphi_i \, y(t-i) + \varepsilon(t) \quad (5)$$

$$y(t) = f(u(t)u(t-1)...u(t-d)y(t-1)y(t-2)...y(t-d-1)) \quad (6)$$

Hence, structure wise, only the size of the input vector **S** is increased to include the delayed inputs and the delayed outputs.

For both network models, band powers of α, β_1, β_2, β_3, γ_1 and γ_2 for channels F_3, F_4, C_3, C_4, O_1, O_2, T3, T_4, P_3 and P4[21] are selected as features for the input vector of the neural network. Hence, the input layer consisted of 60 input neurons (6 bands x 10 channels). The hidden layer consisted of 24 neurons. Output layer consisted of a single neuron. The binary representation of the output value indicated if the features (pertaining to one of the five pictures shown) which was presented to the network were associated to a 'true' or 'false' condition.

Five different network models were developed in such a way that each network model has the capacity to classify a specific picture shown to the subject. One of the trained networks should therefore be able to identify the subject's perception on one specific visual stimulus among the 5 pictures shown to the subject. Hence, the firing of output neuron in network 1 indicates that the subject is perceiving image 1 and would not fire if the subject perceives the images 2/3/4/5. Likewise, the firing of output in network 2 indicated the subject is being shown Image 2 and accordingly for other Images: 3, 4 and 5.

To ensure that the network possess generalization capability, the samples are cross validated whilst training the neural network[38,39]. In other words, the network is trained with only a portion of samples from the data set, while the remaining samples are being used to validate and test the robustness of the network. The network's performance is validated after each training iteration to avoid over fitting. This is known as early stopping condition whereby if the error of validation increase while training error decreases, then training stops before convergence. 75 percent of samples (390 samples) are randomly selected for training. From the remaining 30 percent of the samples, 15 percent of the samples (78 samples) are randomly selected and used for validation and the balance 15 percent of the samples (78 samples) are used for testing the network model.

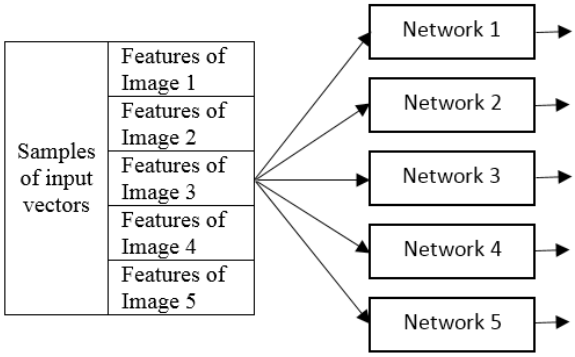

Figure 7. Structure of arrangement of MLP network models. Each network is responsible to identify the subject's perception on 1 of the 5 images shown.

3. Results and Discussions

Table 1 and Table 2 below shows the average accuracy of the trained neural networks on the samples of features representing the EEG signals recorded from 10 subjects. Table 1 shows the accuracy of the trained MLP networks while Table 2 shows the results of the trained NARX network. From the results, it can be observed that the NARX model has the highest overall classification accuracy of 98.1%, whereas the MLP model has the highest overall classification accuracy of 93.3%. From which it is evident that the NARX model has performed better than the MLP model. This reconfirms that EEG signal is a non-stationary signal where the statistical properties of the signal changes over time, where NARX model was designed to capture the changes of features across time with its feedback loop.

The performance of the two network models were then compared based on their sensitivity and specificity values. NARX model's sensitivity performance is significantly

Table 1. Total results of subject 1-10 of MLP network model

Pictures	Training (%)			Validation (%)			Testing (%)			Overall (%)		
	Sensitivity	Specificity	Accuracy	Sensitivity	Specificity	Accuracy	Sensitivity	Specificity	Accuracy	Sensitivity	Specificity	Accuracy
1	98.8	98.8	98.8	74.7	93.8	89.7	69.7	91.2	87.3	90.8	96.9	95.7
2	88.7	97.9	96.1	49.8	91.9	81.8	51.5	91.0	83.1	77.3	96.0	92.0
3	85.7	99.8	97.1	52.9	93.2	84.0	54.2	90.9	83.0	76.0	97.4	93.0
4	90.7	99.4	97.7	57.0	91.2	84.4	52.2	92.6	84.4	79.8	97.2	93.7
5	88.5	98.1	96.3	65.2	89.8	83.8	50.1	87.0	79.8	79.3	95.2	91.9
Mean	90.5	98.8	97.2	59.9	92.0	84.7	55.5	90.5	83.5	80.6	96.5	93.3

Table 2. Total results of subject 1-10 of Narx network model

Pictures	Training (%)			Validation (%)			Testing (%)			Overall (%)		
	Sensitivity	Specificity	Accuracy	Sensitivity	Specificity	Accuracy	Sensitivity	Specificity	Accuracy	Sensitivity	Specificity	Accuracy
1	96.3	99.2	98.4	90.9	97.5	96.0	97.1	96.6	96.7	95.6	98.5	97.9
2	97.5	99.6	99.2	96.5	97.5	97.3	90.3	98.0	96.6	96.2	99.0	98.5
3	95.5	99.3	98.5	92.2	95.9	95.2	91.9	96.9	96.0	94.4	98.4	97.7
4	94.6	99.1	98.3	93.0	96.9	95.6	88.8	98.1	96.4	93.6	98.6	97.6
5	96.1	99.4	98.7	92.4	97.1	96.0	91.9	97.0	96.3	95.0	98.6	98.0
Mean	96.9	99.5	99.0	89.3	97.8	96.1	91.3	95.6	95.9	95.2	98.4	98.1

higher when compared to that of MLP model (95.6% compare to 80.6%). In other words, the trained MLP have higher tendency to produce an error when presented with a 'true' condition for the feature of an image.

From the accuracy of validation and testing, we can also deduce that NARX network models have better generalization capability compare to MLP model. While validation and testing data sets are not used to train the network, we can know if patterns of the features are appropriately learnt by the network instead of resulting in over fitting. NARX model also have significantly higher testing and validation accuracy (testing: 95.9%, validation: 96.1%) when compared with the MLP's model (testing: 83.5%, validation: 84.7%). From the average results from 10 subjects, it can be observed the MLP model has a lower generalization capability when compared to the NARX model though the MLP model has yielded higher classification accuracy during training but dropped while testing with the untrained samples.

Henceforth, we can conclude that NARX model is better suited for classifying EEG signals associated to the mental task of visual perception. Since both models are trained with the same training algorithm (LM), hence we can say that NARX models have higher generalization capability, higher sensitivity and higher accuracy compare to MLP models.

4. Conclusion

As a conclusion, the proposed method can be used as a system for a BCI, implemented to control a semi-autonomous wheelchair. The shared control between the operator and the supporting navigational system is a means to reduce the number of task the user has to perform to reach a destination. By displaying five pictures to the user, the user will determine which location he wants to go to by concentrating on a specific image. Hence this system can be implemented on point-to-point navigation.

Such a design can be used alongside with a BCI system with precision control. Compared to the proposed visual perception approach, a system with precision control requires its user to continuously input command for every execution of action. For instance, if the BCI system is designed by using motor imagery as control signal, the user have to image the task for forward, backward and stop or turning left or right continuously to navigate about in an area to reach a targeted destination. This control method is good for short distance navigation of a few metres with few obstacles along the path but demand its users for continuous concentration. Hence, implementing both systems together means that the operator would have the flexibility to switch between visual perception

control for room-to-room navigation and to use motor imagery for inter-room navigation.

5. Acknowledgement

The authors would like to give thanks to Y. Bhg. Kol. Prof. Dato' Dr. Kamarudin B. Hussin, Vice Chancellor, University Malaysia Perlis for his constant encouragement and support of this research.

6. References

1. Wolpaw JR, et al. Brain-computer interface technology: A review of the first international meeting. IEEE transactions on rehabilitation engineering. 2000 Jun; 8(2): 164–73.
2. Cheng M, et al. Design and implementation of a brain-computer interface with high transfer rates. IEEE Transactions on Biomedical Engineering. 2002 Oct; 49(10):1181–6.
3. Allison BZ, et al. Towards practical brain-computer interfaces: Bridging the gap from research to real-world applications. Springer Science and Business Media; 2012.
4. Leigh PN, Ray-Chaudhuri K. Motor neuron disease. Journal of Neurology, Neurosurgery and Psychiatry. 1994; 57(8):886.
5. Patterson JR, Grabois M. Locked-in syndrome: A review of 139 cases. Stroke. 1986 Jul-Aug; 17(4):758–64.
6. Clark J, Pritchard C, Sunak S. Amyotrophic Lateral Sclerosis: A report on the state of research into the cause, cure and prevention of ALS. June 2005.
7. Anupama HS, Cauvery NK, Lingaraju GM. Brain computer interface and its types - A study. International Journal of Advances in Engineering and Technology. 2012 May; 3(2):739–45.
8. Hema CR, Yakoob S, Nagarajan R, Adom AH, Paulraj MP. EEG based brain machine interface for rehabilitation: A tour guide. 3rd Kuala Lumpur International Conference on Biomedical Engineering; 2006 Dec. p. 632–6.
9. Yuksel BF, Donnerer M, Tompkin J, Steed A. Novel P300 BCI interfaces to directly select physical and virtual objects. 2011; 1–4.
10. Montesano L, Diaz M, Bhaskar S, Minguez J. Towards an intelligent wheelchair system for users with cerebral palsy. IEEE Transactions on Neural Systems and Rehabilitation Engineering. 2010 Apr; 18(2):193–202.
11. Iturrate I, Antelis J, Minguez J. Synchronous EEG brain-actuated wheelchair with automated navigation. Robotics and Automation. 2009 May; 2318–25.
12. Mandel C, Luth T, Laue T, Rofer T, Graser A, Krieg-Bruckner B. Navigating a smart wheelchair with a brain-computer interface interpreting steady-state visual evoked potentials. Intelligent Robots and Systems. 2009 Oct:1118–25.
13. Bourke T. Development of a Robotic Wheelchair. 2011 Nov: p. 1–10.
14. Fehr L, Langbein WE, Skaar SB. Adecuacy of power wheelchair control interfaces for persons with severe disabilities: A clinical survey. Journal of Rehabilitation Research and Development. 2000 May/Jun; 37(3):353–60.
15. John-Dylan H, Rees G. Decoding mental states from brain activity in humans. Nature Reviews Neuroscience. 2006 Jul; 7(7):523–34.
16. Melissa Z, et al. The effect of connectivity on EEG rhythms, power spectral density and coherence among coupled neural populations: Analysis with a neural mass model. IEEE Transactions on Biomedical Engineering. 2008 Jan; 55(1):69–77.
17. Smith SJM. EEG in the diagnosis, classification, and management of patients with epilepsy. Journal of Neurology, Neurosurgery and Psychiatry. 2005 Jun; 76(S2).
18. Fitzgibbon SP, et al. Removal of EEG noise and artifact using blind source separation. Journal of Clinical Neurophysiology. 2007 Jun; 24(3):232–43.
19. Barlow JS. Methods of analysis of nonstationary EEGs, with emphasis on segmentation techniques: A comparative review. Journal of Clinical Neurophysiology. 1985 Jul; 2(3):267–304.
20. Barry SM. Basic concepts and clinical findings in the treatment of seizure disorders with EEG operant conditioning. Clinical EEG and Neuroscience. 2000 Jan; 31(1):45–55.
21. Kim KH, Kim JH. Analysis of induced gamma-band activity in EEG during visual perception of Korean, English, Chinese words. Neuroscience letters. 2006 Aug; 403(3):16–21.
22. Lochy A, Van Belle G, Rossion B. A robust index of lexical representation in the left occipito-temporal cortex as evidenced by EEG responses to fast periodic visual stimulation. Neuropsychologia. 2015 Jan; 66:18–31.
23. Wilamowski BM. Neural network architectures and learning algorithms. IEEE Industrial Electronics Magazine. 2009 Dec; 3(4):56–63.
24. Hema CR, Paulraj MP, Yaacob S, Adom AH, Nagarajan R. An analysis of the effect of EEG frequency bands on the classification of motor imagery signals. Biomedical Soft Computing and Human Sciences. 1995; 16(1):121–6.
25. Zhang GP. Neural networks for classification: A survey. Systems, Man and Cybernetics, Part C: applications and reviews. 2000 Nov; 30(4):451–62.
26. Capilla A, Pazo-Alvarez P, Darriba A, Campo P, Gross J. Steady-state visual evoked potentials can be explained by temporal superposition of transient event-related responses. PLoS One. 2011 Jan; 6(1):e14543.

27. Dentico D, et al. Reversal of cortical information flow during visual imagery as compared to visual perception. NeuroImage. 2014 Oct; 100:237–43.
28. Kiymik MK. et al. Comparison of STFT and wavelet transform methods in determining epileptic seizure activity in EEG signals for real-time application. Computers in Biology and Medicine. 2005 Oct; 35(7):603–16.
29. Hornik K, Stinchcombe M, White H. Multilayer feed forward networks are universal approximators. Neural Networks. 1989; 2(5):359–66.
30. Teplan M. Fundamentals of EEG measurement. Measurement Science Review. 2002; 2(2):1–11.
31. Gross H, et al. Human eye. Handbook of Optical Systems: Survey of Optical Instruments. Wiley-VCh; 2005.
32. Hekin M. ANN-based classification of EEG signals using the average power based on rectangle approximation window. Electrical Review. 2012 Aug; 88:210–5.
33. Riedmiller M. Advanced supervised learning in multi-layer perceptron's–from back propagation to adaptive learning algorithms. Computer Standards and Interfaces. 1994; 16(3):265–78.
34. Saduf MAW. Comparative study of back propagation learning algorithms for neural networks. International Journal of Advanced Research in Computer Science and Software Engineering. 2013 Dec; 3(2):1151–6.
35. Nawi NM, Khan A, Rehman MZ. A new Levenberg Marquardt based back propagation algorithm trained with Cuckoo search. Procedia Technology; 2013. p. 18–23.
36. Ananth R. The Levenberg-Marquardt algorithm. Tutorial on LM Algorithm. 2004 Jun; 1–5.
37. Hagan MT, Menhaj MB. Training feed forward networks with the Marquardt algorithm. IEEE Trans on Neural Networks Sciences. 1994 Nov; 5(6):989–93.
38. Wada Y, Kawato M. Estimation of generalization capability by combination of new information criterion and cross validation. IJCNN-91-Seattle International Joint Conference on Neural Networks; 1991 Jul 8-14. p. 1–6.
39. Prechelt L. Automatic early stopping using cross validation: quantifying the criteria. Neural Networks. 1998 Jun; 11(4):761–7.
40. Naderi MA, Mahdavi-Nasab H. Analysis and classification of EEG signals using spectral analysis and recurrent neural networks. IEEE 17th Iranian Conference of Biomedical Engineering (ICBME); 2010 3-4 Nov.
41. Kato H, Taniguchi M, Honda M. Statistical analysis for multiplicatively modulated nonlinear autoregressive model and its applications to electrophysiological signal analysis in humans. IEEE Transactions on Signal Processing. 2006 Sep; 54(9):3414–25.
42. Siegelmann HT, Bill GH, Giles CL. Computational capabilities of recurrent NARX neural networks. IEEE Transactions on Systems, Man and Cybernetics, Part B: Cybernetics. 1997 Apr; 27(2):208–15.